Intermediate valence behavior in the new ternary compound $Yb_{13}Pd_{40}Sn_{31}$

R.F. Djoumessi[1], A.M. Strydom[1], F. Gastaldo[2], I. Čurlík[3,] M. Reiffers[3], and M. Giovannini[2]

[1] Highly Correlated Matter Research Group, Physics Department, University of Johannesburg, PO Box 524, Auckland Park 2006, South Africa
[2] Department of Chemistry, University of Genova, Via Dodecaneso 31, 1-16146 Genova, Italy
[3] Faculty of Humanities and Natural Sciences, University of Prešov, 17. Novembra 1, SK 081 16 Prešov, Slovakia

E-mail: amstrydom@uj.ac.za

Abstract. The new compound $Yb_{13}Pd_{40}Sn_{31}$ crystallizes in a hexagonal structure of space group P6/mmm (number 191). Magnetic susceptibility shows a non-regular temperature dependence for a local-magnetic moment system. The inverse magnetic susceptibility does not obey Curie-Weiss law throughout the measured temperature range (400 K - 2 K). This behavior is unexpected for Yb in its magnetic Yb^{3+} state and suggests that the system is subject to valence instabilities such as c-f hybridization. We find that the magnetism in $Yb_{13}Pd_{40}Sn_{31}$ is well described by the interconfiguration fluctuation (ICF) model, having an unstable valence for the Yb ion. The temperature dependent electrical resistivity shows that the compound becomes superconducting below 2.3 K. Specific heat analysis shows a peak at 2.3 K indicative of bulk superconductivity, and that the anomaly at 2.3 K survives even in 1 T but becomes suppressed in B = 4 T. As an important discovery, we observe that, aside from the peak at T_c, there is an enormous upturn in the electronic specific heat well below T_c which may be precursor effect of very low-lying magnetic order.

1. Introduction

Rare-earth intermetallic based materials are the most intriguing and thoroughly studied among the strongly correlated electron systems. The proximity of the 4f shell to the Fermi level leads to peculiar phenomena such as heavy fermion behavior, non-Fermi liquid behavior, Kondo effect, valence fluctuation and superconductivity to name a few. Those characteristics are mainly believed to arise due to a variable hybridization between the localized 4f-electrons and the delocalized conduction electrons. In particular and in contrast to cerium, ytterbium-based intermetallics are much less studied due to the high vapor pressure of elemental ytterbium making the sample preparation extremely difficult therefore limiting discovery of new materials; but their correlated electron physics are no less exciting. The most intensively studied systems of the intermediate valence state are cerium based. The Yb compound of this work is an extension to the series of already known Yb-based intermediate valence systems [1, 2]. We report on the magnetic and physical properties of the new ternary intermetallic compound $Yb_{13}Pd_{40}Sn_{31}$ obtained as part of the investigation of the isothermal section of the Yb-Pd-Sn system at 600°C [3].

2. Synthesis and experimental details

Stoichiometric amounts of the reactants Yb (99.9 wt-%), Pd (99.95 wt-%) and Sn (99.999 wt-%) were mixed together to form a polycrystalline sample of $Yb_{13}Pd_{40}Sn_{31}$ by induction melting in a sealed tantalum crucible under a stream of pure argon. To improve the homogeneity, the obtained sample was then wrapped in Ta foil, placed in an evacuated quartz tube and annealed in a furnace at 600°C for 14 days. It was subsequently quenched in cold water. The microstructure of the sample was obtained from the semiquantitative analysis using quantitative Electron Probe MicroAnalysis (EPMA) and Scanning Electron Microscopy (SEM). X-ray diffraction was used for phase identification of crystalline materials and to establish microscopic details such as chemical phase purity, crystallographic lattice parameters as well as details of the atomic coordinates in the structural unit cell. The experiment was carried out on an X'Pert MPD diffractometer and the collected data analyzed using the Powder-Cell [4] program.

Magnetic susceptibility and magnetization measurements were performed on a 7 T SQUID magnetometer (MPMS XL, Quantum Design, San Diego) in the temperature range of 1.7 K - 400 K. Electrical resistivity measurements in the temperature range between 1.8 and 300 K were performed based on the four-probe method using the Electrical Transport Option (ETO) available on the commercial Physical Property Measurement System (PPMS) from the same manufacturer. This latter facility was used also for the heat capacity measurements based on the quasi-adiabatic time relaxation method.

3. Results and Discussion

The powder X-ray diffraction pattern indicated that the obtained sample was single-phase, and crystallizes in a hexagonal structure, similar to hP168-$Y_{13}Pd_{40}Sn_{31}$ as already reported in [3]. The magnetic and physical properties of $Yb_{13}Pd_{40}Sn_{31}$ are investigated for the first time and reported in this work. The magnetic susceptibility will be analyzed in two temperature regions, using two different models, which is justified due to the temperature evolution of χ that is non-monotonous.

Figure 1 shows the DC-magnetic susceptibility measured in a field-cooling mode in an applied magnetic field of 0.01 T. Between 400 K and 60 K, $\chi(T)$ is found to be only very weakly temperature dependent. Most importantly, there is no Curie-Weiss behavior as we would expect if the Yb ion was in its stable magnetic Yb^{3+} state. This effect could be intrinsic and due to a magnetic moment instability of the Yb^{3+} ions, such as what Ce and Yb correlated electrons systems are prone to. The origin of this can be a crystalline electric field (CEF) effect or a strong and temperature dependent moment screening effect known as Kondo effect. However, the inverse magnetic susceptibility ranging from about 10 K down to the lowest measured temperature can be adequately described by a modified Curie-Weiss law as shown in the inset of figure 1 given by the expression:

$$\chi(T) = \frac{N_A \mu_{eff}^2}{3k_B(T - \theta_P)} + \chi_0, \tag{1}$$

where N_A is the Avogadro number and k_B the Boltzmann constant. μ_{eff} and θ_P are respectively the effective magnetic moment and the Weiss temperature and χ_0 is the temperature-independent susceptibility. The least-squares fit of equation 1 leads to $\theta_P = -0.70(2)$ K, $\chi_0 = 1.6 \times 10^{-3}(3)$ emu/mol.Yb and $\mu_{eff} = 0.50\ \mu_B$/Yb. While the negative value of the Weiss temperature suggests the presence of some weak antiferromagnetic interactions, the strongly reduced value of the effective moment compared to the value of the free $Yb^{3+} = 4.54\ \mu_B$ suggests a strong hybridization between the 4f and conduction electrons. Evidently below$\sim$10 K, this system achieves a stable but strongly renormalized magnetic moment. The higher-temperature situation is described below.

The mid-to higher temperature region magnetic behavior of the Yb ions can be well understood

in terms of the Interconfiguration fluctuation (ICF) model [2, 5] between $4f^{13}$ and $4f^{14}$ states of Yb described by the equation:

$$\chi_{\rm ICF}(T) = \frac{{\rm N_A}\mu_{\rm eff}^2(1-\nu(T))}{3{\rm k_B}(T+T_{\rm sf})}, \qquad \text{with} \qquad \nu(T) = \frac{1}{1+8\exp[-E_{ex}/{\rm k_B}(T+T_{\rm sf})]}, \tag{2}$$

where $\nu(T)$ is the fractional occupation of the $4f^{14}$ electronic ground state of the Yb compounds. E_{ex} represents the energy difference between respectively the ground state ($4f^{14}$, Yb^{2+}) and the excited state ($4f^{13}$,Yb^{3+}). $T_{\rm sf}$ is the spin fluctuation temperature that gives an estimation of the width of the 4f-level after the hybridization process with the conduction electrons. $\nu(T)$ describes the $4f^{13} \rightleftharpoons 4f^{14}$ valence instability in the Yb ion as a conduction electron effectively jumps into the 4f-shell momentarily due to the electron affinity to fill the shell. This is permitted to happen as a consequence of overlapping wave functions. The ground state ($4f^{14}$, Yb^{2+}) has both zero angular momentum and effective magnetic moment and the excited state ($4f^{13}$,Yb^{3+}) corresponds to the total angular momentum $J = 7/2$ and an effective magnetic moment $\mu_{\rm eff} = 4.54\ \mu_{\rm B}$. The least-squares fit of the data in the temperature range 10 to 400 K can be done by the following formula:

$$\chi(T) = \chi_{\rm ICF}(T) + \chi_{\rm imp}(T) + \chi_0, \tag{3}$$

where $\chi_{\rm imp}(T) = C_{\rm imp}/(T+\theta_{\rm imp})$ is the Curie-Weiss impurity and χ_0 comes from the temperature-independent contributions that is the Van Vleck paramagnetism and the core electron diamagnetism. This produces results as shown by the fit in figure 2. The least-squares

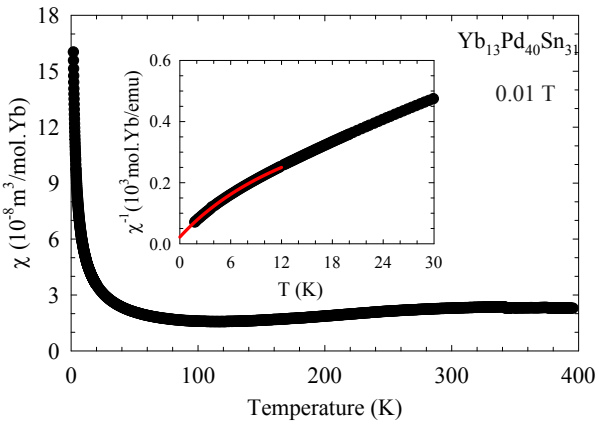

Figure 1. Temperature dependence of the magnetic susceptibility $\chi(T)$ measured up to 400 K. The inset represents the least-squares fit of equation 1 to the low-region of $\chi(T)$ with parameters as discussed in the text.

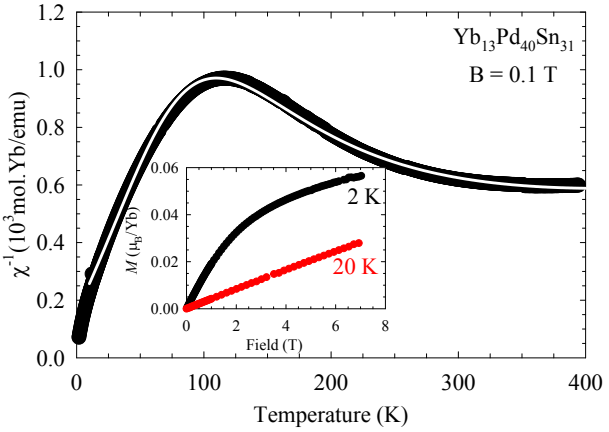

Figure 2. Temperature dependence of the inverse magnetic susceptibility $\chi^{-1}(T)$. The solid line represents the ICF fit of equation 3 as discussed in the text. Inset: magnetization isotherms in fields up to 7 T.

fit leads to the parameters: $C_{\rm imp} = 0.128$ emu.K/Yb.mol; $\theta_{\rm imp} = -18.9$ K; $E_{\rm ex} = 1306$ K; $T_{\rm sf} = 173$ K and $\chi_0 = 6.33 \times 10^{-4}$ emu/mol.Yb. The value of the spin fluctuation temperature is in qualitative agreement with the position of the peak on the experimental data. In the inset of figure 2, the isothermal magnetization has been measured in fields up to 7 T for two different temperatures, 2 and 20 K. At 2 K, the magnetization shows a curvature as B increases together with a tendency to saturate at high fields while at 20 K, we observe a linear in B behavior as expected for a paramagnetic system with $T < T_{\rm sf}$. From these measurements, there is no

evidence of a magnetic phase transition down to the lowest measured temperature.
The temperature dependence of the electrical resistivity in zero applied magnetic field is presented in figure 3. The compound reveals a quasi-metallic like behavior in a broad temperature range. A superconducting phase transition is observed at about 2.2 K with a critical field of ≈ 50 mT when $T = 0.4$ K (not shown here). However, the bulk character of this superconductivity behavior has not been fully proven yet and more susceptibility measurements are planned. Below about 10 K, the data follows the Fermi-liquid relation where the electron-phonon scattering is taken into account as shown in the following equation:

$$\rho(T) = \rho_0 + \rho_{ee}T^2 + \rho_{ep}T^5, \tag{4}$$

where ρ_0 is the residual resistivity, ρ_{ee} and ρ_{ep} the parameters that account respectively for the electron-electron and the electron-phonon scattering. The least-squares fit as shown in

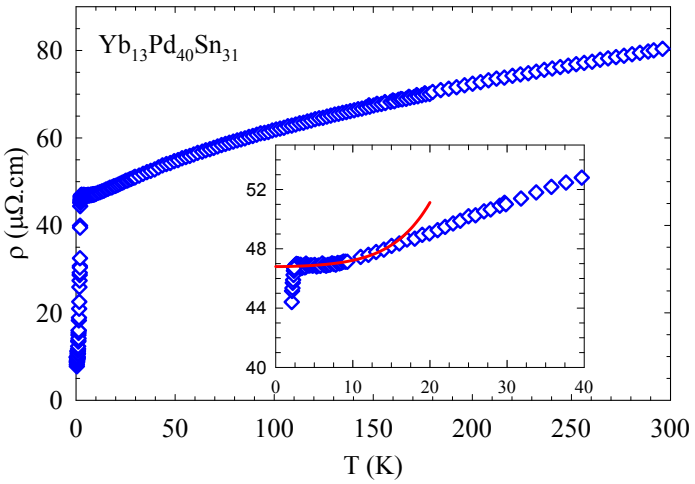

Figure 3. Temperature dependence of electrical resistivity. Inset: Low temperature region with a least-squares fit of the Fermi-liquid relation.

the inset yields to the parameters $\rho_0 = 46.80$ $\mu\Omega$.cm, $\rho_{ee} = 3.3 \times 10^{-3}$ $\mu\Omega$.cm. K^{-2} and $\rho_{ep} = 9.4 \times 10^{-7}$ $\mu\Omega$.cm K^{-5}.
Figure 4 shows the temperature dependence of heat capacity. As observed in figure 4(a), the superconducting phase transition observed in the electrical resistivity is also present here and moreover, it appears that the anomaly at ≈ 2.2 K survives even in 1 T but becomes completely suppressed in 4 T. This suggests a field driven dynamic besides the superconductivity. Quite aside from the peak at the transition, there is an enormous upturn in $C_p(T)/T$ towards lowest temperature that could be at a first thought a form of nuclear entropy originating from a hyperfine splitting. It is noted that among the highest natural abundance, the ^{171}Yb isotope has a I = 1/2 nuclear spin while ^{173}Yb isotope has a I = 5/2. However, the behavior in a field of 1 T is not consistent with the evolution of the tail at low temperature in the case of a nuclear contribution to the heat capacity. The entropy was estimated from the relation:

$$S(T) = \int_0^T \frac{C_P(T')}{T'} dT' \tag{5}$$

The data as represented in (b) shows no tendency to saturation in the entropy and a rather weak field dependence associated with a power law behavior. As presented in (c), the low-temperature data of $C_P(T)/T$ data shows a linear dependence in T^2 corresponding to the

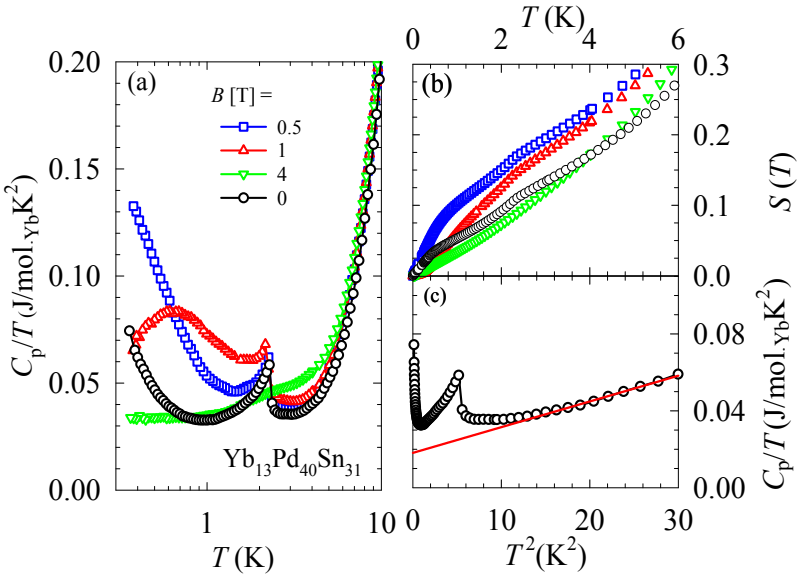

Figure 4. (a): Temperature dependence of the heat capacity for different applied magnetic fields. (b): Calculated entropy in different applied fields. (c): Low temperature region of the C_p/T vs T^2 dependence in zero field with a fit of the most linear region as discussed in the text.

electronic contribution to the specific heat. This gives an estimate of the Sommerfeld coefficient that is found to be $\gamma = 18.1$ mJ/mol.K^2. From this value we can say that the effective mass $m^* \simeq 3m_e$(free electron mass) [6], which is a slightly enhanced value indicating the presence of some electronic correlations but it is still low to classify the compound $Yb_{13}Pd_{40}Sn_{31}$ as a heavy fermion system where the effective mass can be up to thousand times more than the mass of a free electron [6].

4. Conclusion

In summary, the new Yb ternary compound $Yb_{13}Pd_{40}Sn_{31}$ that crystallizes in hexagonal structure is found here to be a new intermediate valence system with no magnetic ordering from the magnetic susceptibility, electrical resistivity and heat capacity results. Moreover, a superconducting behavior that remains to be investigated is also consistently found in the low-temperature measurements of the electrical resistivity and heat capacity.

Acknowledgments

RFD thanks UJ for a scholarship and both the research group members and Dr. M. Falkowski from the Charles University in Prague for their help and fruitful discussions. AMS thanks the FRC/URC of UJ and the SA NRF (93549) for financial assistance.

References

[1] Kaczorowski D, Gribanov A, Rogl P and Dunaev S 2016 *J. Alloys Comp.* **685** 957–961

[2] Kowalczyk A, Falkowski M and Toliński T 2010 *J. Appl. Phys.* **107** 123917

[3] Gastaldo F, Giovannini M, Strydom A, Djoumessi R, Čurlík I, Reiffers M, Solokha P and Saccone A 2017 *J. Alloys Comp.* **694** 185–192

[4] Kraus W and Nolze G 1996 *J. Appl. Cryst.* **29** 301–303

[5] Sales B and Wohlleben D 1975 *Phys. Rev. Lett.* **35** 1240

[6] Kittel C 1996 *Introduction to Solid State Physics* (Wiley, New York)